Adsorption (2012) 18:31–42
DOI 10.1007/s10450-011-9378-7

Adsorption of benzene and propene in zeolite MCM-22: a grand canonical Monte Carlo study

Peng He · Hui Liu · Yanfeng Li · Jiqin Zhu · Shiping Huang · Zhigang Lei · Peng Wang · Huiping Tian

Received: 20 February 2011 / Accepted: 14 September 2011 / Published online: 28 September 2011

Abstract The GCMC (grand canonical Monte Carlo) simulation technique was used to predict the competition adsorption characteristics of benzene and propene in different pore systems of MCM-22. The nine-site model of benzene was used, which proved to be effective and efficient. The zeolite was divided into three adsorption sites following a simulated annealing method. It is found that benzene and propene have the same preferential adsorption site and a similar adsorption order in different sites. Moreover, the pure and mixture isotherms of the three sites are drawn. From the isotherms, we obtained a selectivity reversal of the mixture isotherms of benzene and propene in different sites. It is also noted that the competition adsorption in the three adsorption sites for the two adsorbates can fall into three successive steps and the adsorption order of propene in mixture in these three sites is S3 → S1 → S2. A new model is presented to predict the benzene and propene adsorption equilibrium in MCM-22. This approach yields better multicomponent equilibrium predictions than ideal adsorbed solution theory (IAST). Isotherms at different mole fraction of benzene in gas phase indicate an advantage to increase the feed radio of benzene and propene. Thus, this work is helpful for a better understanding of the adsorption mechanism of benzene and propene in MCM-22 and hence the relation of the catalytic properties of the zeolite to its structure.

Keywords MCM-22 zeolite · Benzene alkylation · Selectivity reversal

P. He · H. Liu (✉) · Y. Li · J. Zhu · Z. Lei
State Key Laboratory of Chemical Resource Engineering, Campus Box 35, Beijing, China
e-mail: hliu@mail.buct.edu.cn

S. Huang
Division of Molecular and Materials Simulation, Key Lab for Nanomaterials under Ministry of Education, Beijing University of Chemical Technology, Beijing 100029, China

P. Wang · H. Tian
Research Institute of Petroleum Processing, SINOPEC, Beijing 100083, China

1 Introduction

Zeolites are crystalline microporous materials with well-defined three-dimensional frameworks with channels and/or cavities. Among a wide variety of zeolites, zeolite MCM-22 (IZA structure code MWW) is unique in its framework topology as it has two independent pore systems. One pore system consists of two-dimensional sinusoidal intersecting channels with elliptical 10-member ring (MR) cross sections (4.1 × 5.1 Å). The other system possesses large cylindrical supercages with a diameter defined by a 12-MR (7.1 Å) and a height of 18.2 Å; these supercages are accessible through 10-MR apertures (4.0 × 5.5 Å) (Ayrault et al. 2004). Such a structure renders it attractive when used as ion exchangers (Pawlesa et al. 2007), sorbents (Chen et al. 2001) and catalysts (Jiíejka et al. 2002). As a catalyst in particular, MCM-22 has been found to have high activity for a various range of industrially important reactions involving organic molecules, e.g., catalytic cracking (Zhu et al. 2005), isomerization of paraffins (Asensi et al. 1996) and alkylation of hydrocarbons (Degnan et al. 2001; Perego and Ingallina 2002). In these applications, understanding the relationship between the chemical and catalytic properties of the zeolite and its structure is of particular importance for an effectual design of the catalyst (Hansen et al. 2008a, 2008b).

This paper mainly concerns the adsorption of benzene and propene in the framework of MCM-22, aiming at a first step insight into the alkylation process of benzene with

propene on the active sites of MCM-22. Although the reaction performances of MCM-22 for the benzene alkylation with alkanes and alkenes have been studied extensively by experiment (Jiíejka et al. 2002; Corma et al. 1996, 2000), to our knowledge, the adsorption behaviors of the benzene and/or propene in MCM-22 are not well understood yet in the literature. Experimentally, Fu and Ding (2005) reported data of adsorption heat for benzene/MCM-22, and observed the preferential adsorption of propene in the two-dimensional sinusoidal channels at high loadings. To date, complete experimental adsorption isotherms for the benzene and/or propene in MCM-22 are not available. On the other hand, atomic-level simulations of the adsorption of the system were carried out by several researchers. Using an all-atom model with 12 charged sites, Hou et al. (2001) identified four adsorbing regions for benzene and propene in MCM-22 based on simulation results of pure component adsorption. A significant simulation work by Ban et al. (2007) investigated the adsorption selectivity of benzene/propene in MCM-22 using a nine-site benzene model, and demonstrated the dominant adsorption of benzene over propene in binary propene/benzene mixtures. While some adsorption characteristics of benzene and propene in MCM-22 have been revealed by the few studies, a comprehensive and detailed description of adsorption properties of the system is still wanting.

The objective of the present study is to elucidate the intrinsic inhomogeneity of the MCM-22 structure by identifying different adsorption sites with the probing guest molecules, so as to gain insight into the behavior of adsorption of benzene and propene in MCM-22 qualitatively and quantitatively. Equilibrium data both for single and binary forms are reported and analyzed. In the present work, adsorption sites are distinguished according a simulated annealing method. The GCMC (grand canonical Monte Carlo) simulation technique was used to predict the competition adsorption characteristics of benzene and propene in different adsorption sites of MCM-22. We intended to show the competition adsorption of the two adsorbates and how temperature, pressure, and the feed radio can affect the results. Three-site Langmuir model and the ideal adsorbed solution theory (IAST) (Myers and Prausnitz 1965) were used to fit the pure and mixture isotherms respectively. Finally, a new model was presented, which perform better than IAST in predicting the mixture equilibrium data.

2 Molecular models and simulation methodology

We selected the siliceous, cation-free analogue of MCM-22, ITQ-1, as the host structure of adsorption. ITQ-1 has an unit cell composition of $Si_{144}O_{72}$ in the *P6/mmm* space group with $a = 14.2081$ Å and $c = 24.9452$ Å, as characterized by the neutron diffraction study of Camblor et al. (1998). Benzene and propene were the adsorbates.

In our simulations, both dispersion and Coulombic interactions were taken into account for benzene, while the propene was assumed to interact with the surroundings through dispersion interactions only. The dispersion interactions were described by the (6–12) Lennard-Jones (LJ) model; Table 1 lists the parameters adopted. The Ewald summation was used for the Coulombic interactions, and a cutoff radius of 13 Å was applied for the LJ interactions. The LJ interactions between adsorbates and Si atoms were taken to be zero since the size and polarizability of the Si atoms are much smaller than those of the O atoms. Such a treatment has been justified for similar host-guest systems, e.g., alkanes in silicate (Schenk et al. 2001; Ban et al. 2007).

Benzene was described by the nine-site model of Zhao et al. (2005), Wick et al. (2002). The partial charges of the zeolite atoms ($q_o = -1.025$e, $q_{si} = +2.05$e) were taken from Calero et al. (2004). The adequacy of this model in describing adsorption of benzene in silicate zeolite has been confirmed by Ban et al. (2007). For propene, whilst charged models are available in the literature (Sastre et al. 1999; Hou et al. 2001), in the present work an uncharged united atom model was used, for simplicity and in view of that for GCMC simulation, Liu et al. (2008) and Ban et al. (2007) have proved the applicability and accuracy of this model in

Table 1 Lennard-Jones parameters for guest-guest and guest-host interactions[a]

Molecule	Atom type	σ (Å)	ε/k_B (K)
Propene	CH_3–CH_3	3.76	108.0
	CH_2 (sp2)–CH_2(sp2)	3.68	92.5
	CH–CH	3.73	52.0
	CH_3–O	3.48	93.0
	CH_2(sp2)–O	3.50	82.6
	CH(sp2)–O	3.43	69.0
Benzene	$CH_{benzene}$–$CH_{benzene}$	3.74	53.5
	$CH_{benzene}$–O	3.38	73.0

[a]Interaction parameters for non-identical hydrocarbon groups were calculated using the Jorgensen mixing rules (Jorgensen et al. 1984)

simulating alkanes adsorption in various pure silica zeolites. The parameters for the CH_3–CH_3 and CH_3–O interactions were taken from Calero et al. (2004). The other interaction parameters for propene (LJ interactions, bond bending, and bond stretching) were the same as those used by Jakobtorweihen et al. (2005).

All adsorption calculations were carried out in the grand canonical ensemble at fixed μ, V and T. The technical details of the method could be found elsewhere (Frenkel and Smit 1996; Snurr et al. 1993) and not repeated here. In our simulations, eight unit cells of ITQ-1 ($2 \times 2 \times 2$) were used to construct the simulation box, and periodic boundary conditions were applied. The zeolite atoms were assumed to be rigid. According to Vlugt and Schenk (2002), assuming flexibility results in only very small deviations for the determination of adsorption properties such as adsorption isotherms and Henry coefficients. For the real equilibration of the system under simulation, long production runs of total 3×10^7 steps were performed, in which course a configuration of the system was recorded every 400 steps. The first 1.5×10^7 steps were used for equilibration and not included in the statistic averaging.

To check the adequacy of the methodology we adopted, the isosteric adsorption heat of benzene in silicalite at a loading of four molecules per unit cell was calculated. Our result is shown in Table 2, along with the simulated one by Ban et al. (2007) and the experimental data by Jentys et al. (2006) and Song et al. (2006). We see a good agreement between our result and the others. We then calculated the adsorption energy values of different regions of MCM-22 and compared them with the literature data; see Table 3. The experimental data of Corma et al. (1996) were obtained from the calorimetric study of adsorption of toluene in MCM-22.

Table 2 Comparison of isosteric adsorption heats of benzene in silicalite

Researchers	Isosteric adsorption heat (kJ/mol)
This paper	51.95
Ban et al.	52.00
Experiment[a]	50.00–53.00

[a]Experimental data were taken from Jentys et al. (2006) and Song et al. (2006)

The simulated values of Hou et al. (2001) and Rungsirisakun et al. (2006) were those from GCMC and MD simulations, respectively. It is noted that the force field here used gives agreeable energy values to those by Corma et al. (1996) and Rungsirisakun et al. (2006). In contrast, our adsorption energy value for the supercages differs significantly from that by Hou et al. (2001), which can be attributed to the different force fields adopted. For the simulation of adsorption of benzene in silicate, it has been shown that the 12-site model (12 partial charges) for benzene adsorption in silicate overestimated the adsorption heat value by around 10 kJ (Chen et al. 2007). Hence, the 9-site model here adopted is not only computationally much more efficient than the 12-site model (3 vs. 12 partial charges), but more accurate in predicting the adsorption of benzene in the two zeolites.

3 Results and discussion

3.1 Adsorption of pure components

To identify the adsorption sites for the two guest molecules in the two pore systems of MCM-22, we first divided the accessible pore spaces into subspaces by adopting a method similar to that of Clark et al. (1998). Twenty benzene and sixty propene molecules were used as the probe molecules respectively. A simulated annealing method was used including a canonical Monte Carlo sampling within the search space. During the course, the temperature is gradually decreased, and finally the system approaches a state corresponding to a local minimum of the potential energy hypersurface in an area of the search space. Other possible local energy minima can be found by repeating the annealing process and thereafter be grouped into two corresponding sets to the two pore systems of MCM-22. The results for benzene and propene are shown in Fig. 1. Both benzene and propene molecules are seen to adsorb on identifiable adsorption sites: the first type of site, denoted as S1 site, locates in the bidimensional sinusoidal channels of MCM-22; the second type of site, denoted as S2 site, locates in the "pockets" adjacent to the supercages that include the interconnected regions between two adjacent supercages; and the third, S3 site, lies in the central region of the 12-MR supercages.

Table 3 Comparison of adsorption energies of benzene in different regions of MCM-22

Researchers	Adsorption energy for different regions (kJ/mol)	
	Sinusoidal channel	Supercage
This paper	86.49	47.72
Corma et al. (2000)	80.00	45.00–50.00
Rungsirisakuna et al. (2006)	–	47.81
Hou et al. (2001)	83.36	75.02

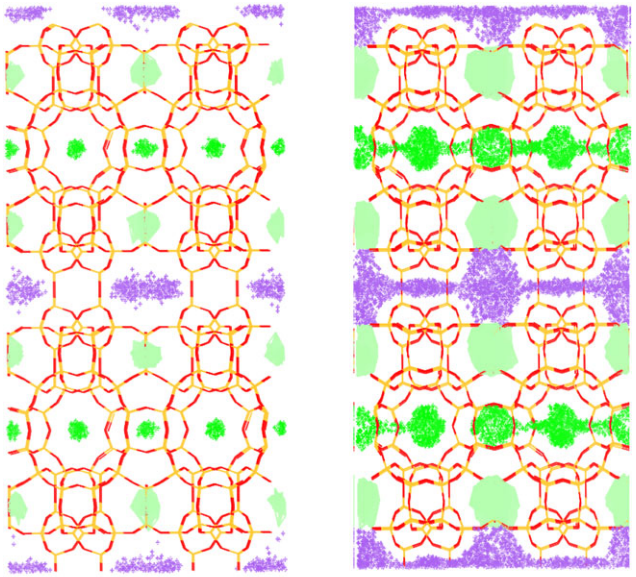

Fig. 1 The accessible sites of (**a**) benzene and (**b**) propene in MCM-22. Sites volumes are shown based on a 50 kJ/mol potential cutoff for the center of mass coordinate of adsorbates. S1 site: *green*; S2 site: *cyan*; S3 site: *purple*

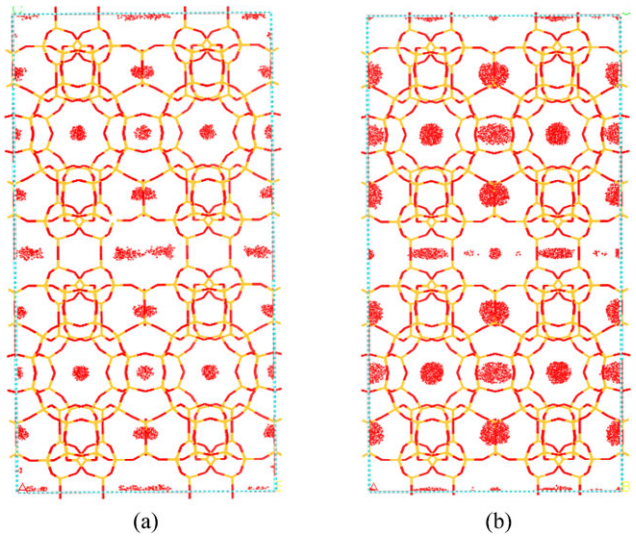

Fig. 2 The center-of-mass distributions in zeolite lattice. (**a**) Benzene; (**b**) Propene

Figure 2 shows typical center-of-mass distributions of the adsorbed benzene and propene in MCM-22, where the center of mass of each adsorbate molecule in each configuration is displayed as dots in the model space. We see that the spatial distributions of the molecules are roughly territorial or segregated (Krishna and Baten 2007). Figure 3 shows the distributions of non-bonding interactions of benzene and propene with MCM-22, respectively. The energy distribution of benzene is three-peaked, with the extremes

Table 4 The adsorption energies of different sites

Components	Adsorption energy (kJ/mol)		
	S1 site	S2 site	S3 site
Benzene	86.49	69.81	47.72
Propene	43.97	38.97	25.22

Table 5 The saturated loadings on different sites

Components	Saturated loadings (molecules/unit cell)		
	S1 site	S2 site	S3 site
Benzene	2	2	3
Propene	4	3	6

being 86.49 kJ/mol, 69.81 kJ/mol and 47.72 kJ/mol, in relation to the three sites S1, S2, and S3, respectively. For propene, there are also three peaks with energy values of 43.97 kJ/mol, 38.97 kJ/mol and 25.22 kJ/mol, respectively. Comparing the peak values for the two adsorbents (see Table 4) shows that the adsorption strength of benzene is stronger than that of propene on the three respective adsorption sites.

Figures 4 and 5 show the adsorption isotherms of benzene and propene at 400 K and 450 K, respectively. For the two adsorbates, a rapid saturation (three molecules per unit cell) in S1 site is observed at very low pressure; then the S2 site is filled; and adsorption starts on S3 site after saturation of both S2 and S1 sites. This is entirely consistent with the hierarchy of magnitudes of the adsorption energies presented in Table 4, which are higher in S1 and S2 sites than that in S3 site. Table 5 presents the saturated loadings in different sites for the two adsorbates, respectively. Although having a stronger adsorption strength than propene (refer to Table 4), fewer benzene molecules are adsorbed on the three sites. This can be attributed to the higher packing efficiency of propene that has a smaller size.

In order to correlate the adsorption isotherms of benzene and propene, the following three-site Langmuir equation was tested

$$\Theta_i^0(P) = \frac{\Theta_{i,A,sat} b_{i,A} P}{1 + b_{i,A} P} + \frac{\Theta_{i,B,sat} b_{i,B} P}{1 + b_{i,B} P} + \frac{\Theta_{i,C,sat} b_{i,C} P}{1 + b_{i,C} P} \quad (1)$$

where P is the pressure of bulk gas at equilibrium with the adsorbed phase, kPa; $\Theta_{i,A,sat}$, $\Theta_{i,B,sat}$ and $\Theta_{i,C,sat}$ are the maximum loadings of component i in sites A, B and C; and $b_{i,A}$, $b_{i,B}$ and $b_{i,C}$ are the corresponding affinity constants. The results are plotted in Figs. 4 and 5. The fitted parameters are listed in Table 6. The good agreement between the fitted and simulated results indicates that the three-site Langmuir

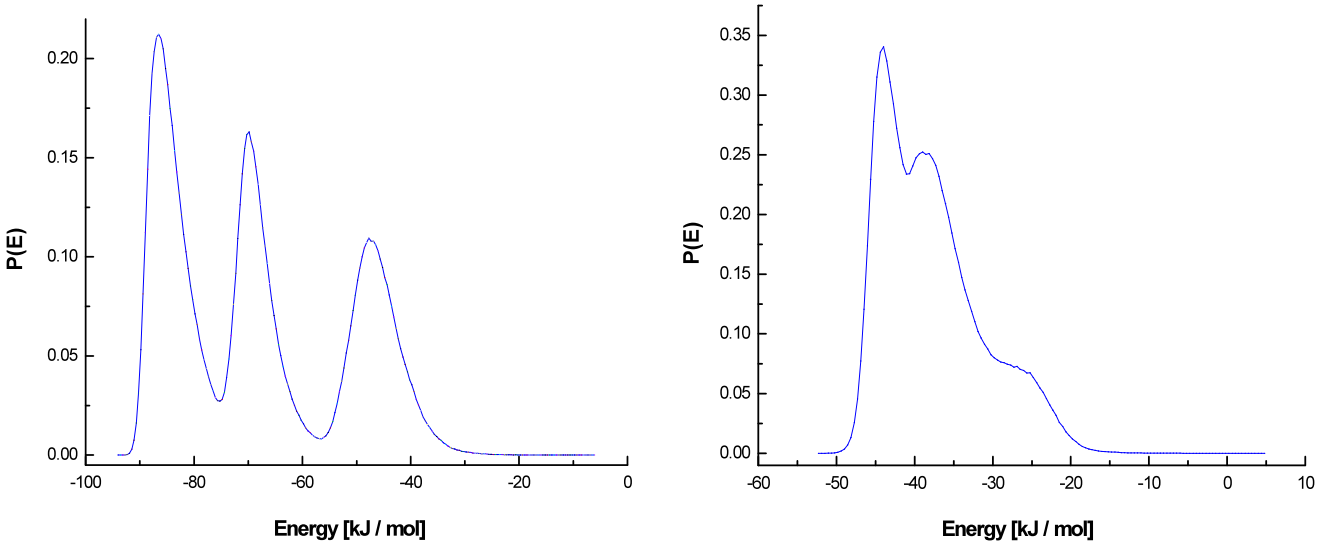

Fig. 3 The adsorbates-zeolite interaction potential energy distribution in zeolite lattice. (**a**) Benzene; (**b**) Propene

Table 6 Pure component parameters for three-site Langmuir model

Components	Temperature (K)	$b_{i,A}$ (kPa^{-1})	$\Theta_{i,A,sat}$ (molecules/ unit cell)	$b_{i,B}$ (kPa^{-1})	$\Theta_{i,B,sat}$ (molecules/ unit cell)	$b_{i,C}$ (kPa^{-1})	$\Theta_{i,C,sat}$ (molecules/ unit cell)
Benzene	400	1.5800	1.30	383.3900	4.70	0.0087	1.10
	450	0.9700	1.60	80.9900	4.10	0.0052	1.00
Propene	400	0.0010	2.45	0.1800	5.07	0.0035	5.33
	450	0.0014	1.74	0.0420	5.14	0.0021	5.27

equation is physically consistent with the three sites nature of the pure component adsorption of benzene and propene in MCM-22.

3.2 Adsorption of binary benzene /propene mixtures

3.2.1 Mixture adsorption isotherm at 400 K

Figure 6 shows the adsorption isotherms of benzene and propene in an equimolar (50/50) mixture at 400 K. In general, a significantly preferential adsorption of benzene over propene is observed over the range of the pressure simulated. Obviously, the energetic advantage of benzene dominates the adsorption process. For benzene, the loading increases continuously up to a pressure of 60 kPa. In this pressure domain, the sequence of benzene adsorption on the three sites follows the hierarchy S1→S2→S3, quite analogous to the sequence in the case of its pure component adsorption. The loading of benzene starts decreasing in excess of 60 kPa, in accompany with decreasing in loadings on all the three sites. For propene, there is no appreciable adsorption below 1 kPa. The loading of propene increases after 1 kPa, mainly arising from its adsorption on the S3 sites that are left unoccupied by the benzene molecules. At higher loadings (higher than 60 kPa), the entropic advantage of the smaller propene molecules then shows up, causing preferential adsorption of propene on the three sites with the hierarchy of sequence S3→S1→S2, which is not in parallel to the adsorption order of pure propene (S1→S2→S3).

3.2.2 The effect of temperature

To show the effect of temperature on mixture adsorption, we additionally computed the binary adsorption isotherms at 360 K and 450 K and compared them with that of 400 K, which is shown in Fig. 7. As seen, below 10 kPa, the loadings of both CO_2 and CH_4 decrease from 360 K to 450 K at the same pressures. With the increase of pressures, an increase in temperature causes the selectivity reversal to occur at a higher value of pressure, i.e., 200 kPa for 360 K and 850 kPa for 400 K. We do not observe a selectivity reversal up to 1000 kPa for 450 K.

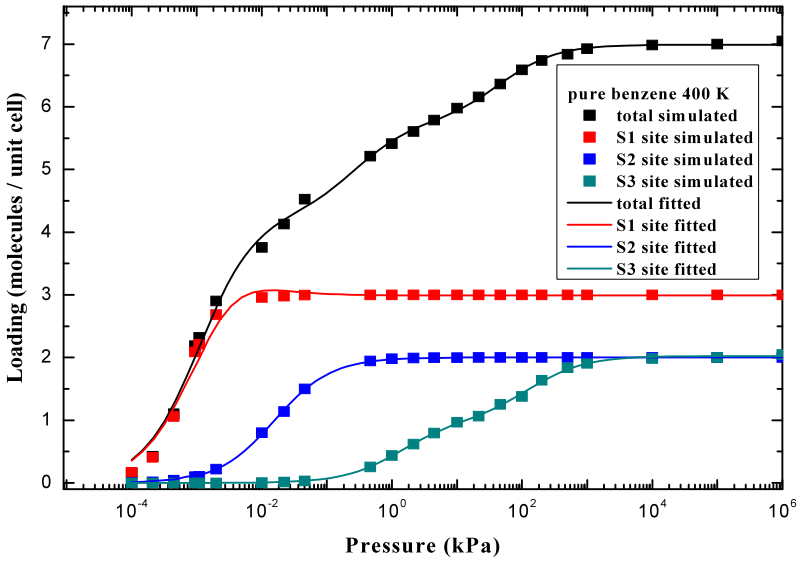

(a)

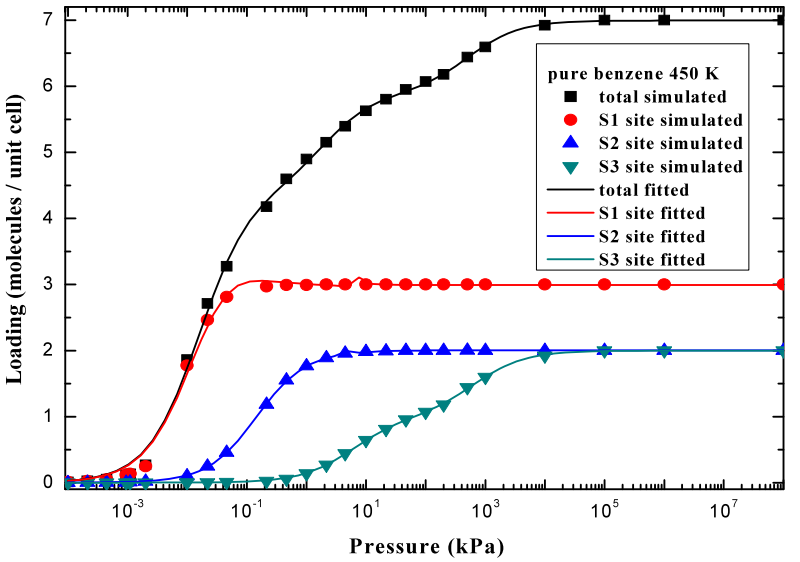

(b)

Fig. 4 Simulated adsorption isotherms of benzene in different regions at (**a**) 400 K; and (**b**) 450 K

3.2.3 The effect of mole fractions of benzene

To show the effect of the mole fractions of benzene on mixture adsorption, Fig. 8 presents the mixture isotherms at 400 K and 1000 kPa at different mole fractions of benzene in the gas phase. It is noticed that the loadings of benzene quickly surpass propene at a relatively lower feed ratio, i.e., 0.10. A carefully examination indicates that selectivity reversal occurs in S1 site at 0.75 and S2 site at 0.60. After the selectivity reversal, benzene molecules quickly displace propene in S1 and S2 sites almost completely. However, for S3 site, to 0.75 that is a higher mole fraction, more benzene molecules adsorb in than propene. Thus, for S3 site, the propene can be located at all mole fraction except the mole fraction of 1.00. According to Fu and Ding (2005), the polymerization of propene will occur when there are more propene molecules than benzene. Our results indicate that it is necessary to increase the mole fractions of benzene to avoid this mainly in S3 site.

3.3 Mixed-gas adsorption equilibria prediction

For practical applications, mixed-gas adsorption equilibria prediction from pure component data is of great importance. Mixed-gas adsorption prediction from pure component data based on the ideal adsorbed solution theory (IAST) (Myers and Prausnitz 1965) has shown better successes (Maurer 1997). However, it has been recognized that failures of IAST predictions may occur due to the treatment

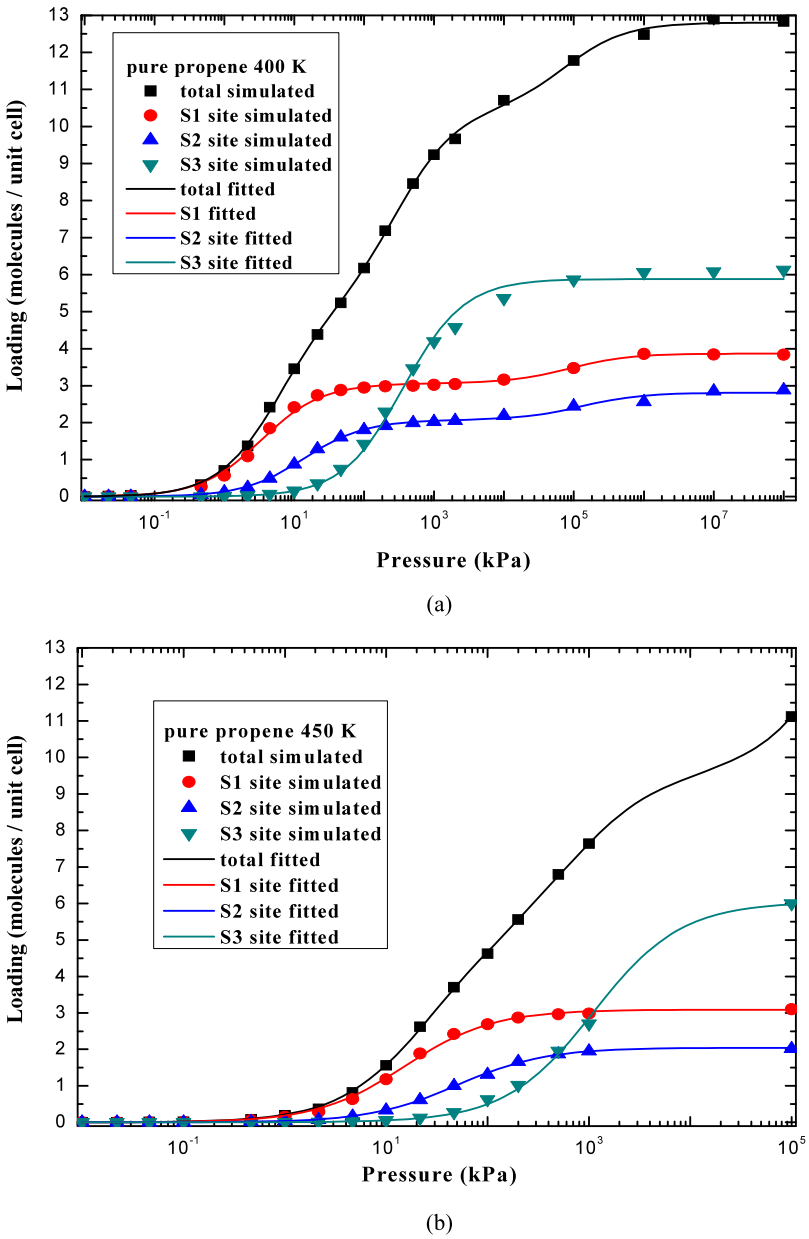

Fig. 5 Simulated adsorption isotherms of propene in different regions at (**a**) 400 K; and (**b**) 450 K

of the adsorbent homogeneous (Myers and Prausnitz 1965; Sircar 1995). From the data of Table 6, the derived IAST data were shown in Fig. 9, which clearly exhibits the failure of the IAST in predicting mixture adsorption of benzene/propene in MCM-22.

The heterogeneous ideal adsorbed solution (HIAST) model employs IAST to evaluate the multicomponent equilibria on each energy site. The overall adsorption equilibria are the integral of the local equilibria over the complete range of energy distribution (Valenzuela and Myers 1998). Gusev and O'Brien (1996) presented a new theory of multicomponent adsorption equilibrium, namely, the multi-space adsorption model (MSAM). The MSAM accounts for the inherent nonuniformity of the adsorbed phase in microporous adsorbents by conceptually dividing the pore volume into distinct "spaces". Then the model predicts multicomponent adsorption equilibrium by applying the IAST separately to each space. This implies treating the spaces as distinct, uniform phases, each independently in equilibrium with the bulk fluid. Maurer (1997) also employed the IAST and a modified Langmuir-Freundlich (LF) model at low and high surface coverage respectively. This approach yields better multicomponent equilibria predictions than IAST-only modeling approaches for many relatively nonideal adsorption systems.

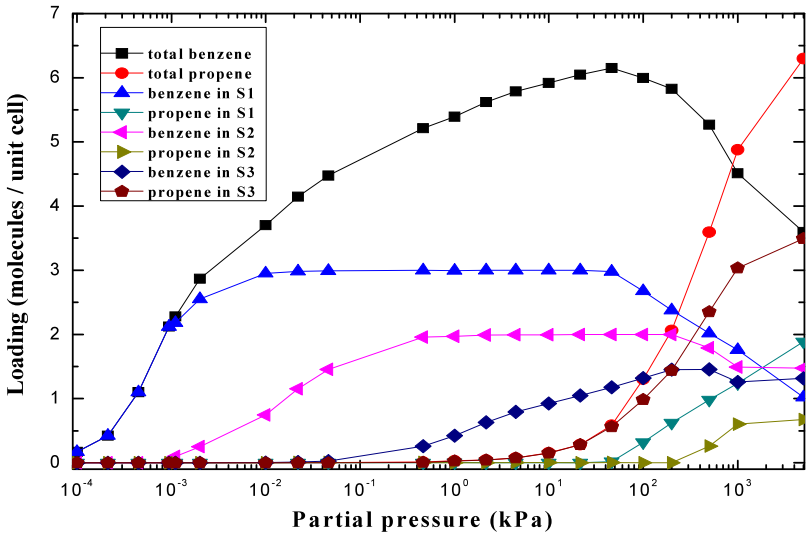

Fig. 6 Adsorption isotherms of benzene and propene in equimolar (50/50) mixtures at 400 K

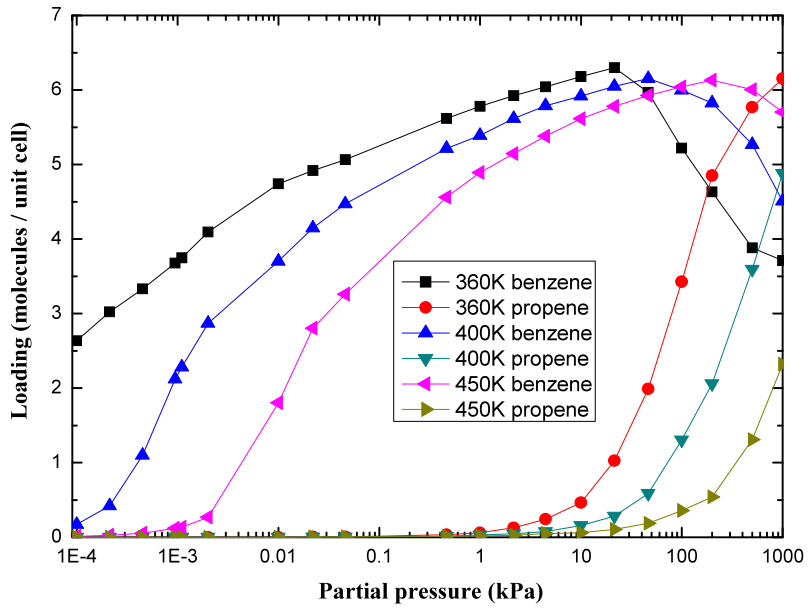

Fig. 7 Adsorption isotherms of benzene and propene in equimolar (50/50) mixtures at different temperatures

The adsorption of benzene and propene in MCM-22 is very energetically heterogeneous in nature with distinct sites or spaces. Therefore, we assume that for different adsorption sites, the IAST is applicable to each site separately.

First, the two-site Langmuir model is used to fit the pure components isotherms of benzene and propene in different adsorption sites.

$$\Theta^{\circ}_{i,j}(P) = \frac{\Theta_{i,A,sat} b_{i,A} P}{1 + b_{i,A} P} + \frac{\Theta_{i,B,sat} b_{i,B} P}{1 + b_{i,B} P} \tag{2}$$

where $\Theta^{\circ}_{i,j}(P)$ is the adsorption amount pure component of species i in site j. Thus, adsorption isotherms in S1, S2 and S3 sites is described by $\Theta^{\circ}_{i,1}(P)$, $\Theta^{\circ}_{i,2}(P)$ and $\Theta^{\circ}_{i,3}(P)$ respectively. The fitted lines are shown in Figs. 4 and 5 at 400 K and 450 K. The fitted parameters are listed in Table 7. The mathematical framework for the IAST calculation in each site is as follows.

Since the adsorption order of propene in mixture in these three regions is S3→S1→S2, which may indicate that the S3 site is the first place that competition adsorption occurs. Thus, the IAST is first applied to S3 site.

The integrated isotherm equations of pure components in S3 site

$$\pi_3 = \frac{RT}{A} \int_{P=0}^{P=P_i^0} \frac{\Theta^{\circ}_{i,3}(P)}{P} dP \tag{3}$$

relates the spreading pressure of site 3, π_3, to the bulk pressure, P_i° (this pressure is used as a standard-state pressure in the mixture calculation), using the pure species isotherms, $\Theta^{\circ}_{i,3}(P)$ (Myers and Prausnitz 1965). Here, A is the adsorbent surface area, R is the universal gas constant, and T is

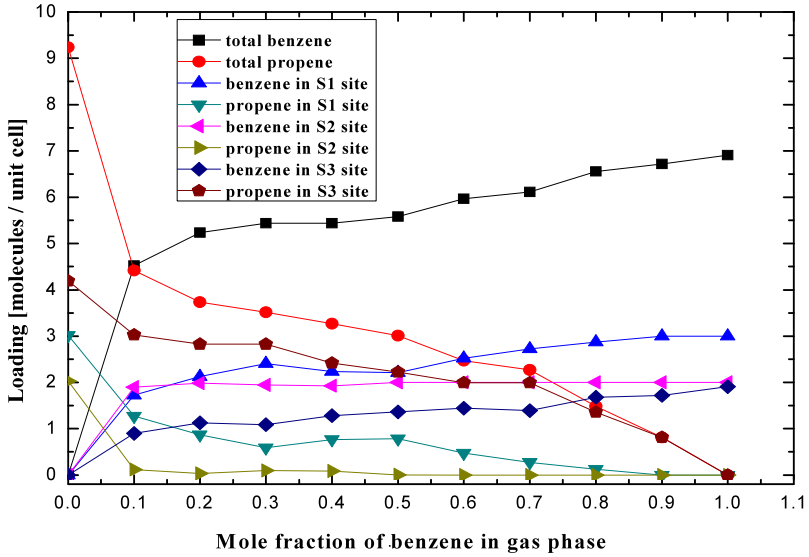

Fig. 8 Loadings of benzene/propene at 400 K, 1000 kPa at different mole fractions of benzene in the bulk phase

Table 7 Pure component parameters for two-site Langmuir models corresponding to S1, S2, S3 sites

Components	Temperature (K)	$b_{i,A}$ (kPa^{-1})	$\Theta_{i,A,sat}$ (molecules /unit cell)	$b_{i,B}$ (kPa^{-1})	$\Theta_{i,B,sat}$ (molecules /unit cell)
S1 site					
Benzene	400	0.0015	0.02	167.4000	3.05
	450	0.0018	0.01	123.9900	3.03
Propene	400	0.2971	3.06	0.0001	0.80
	450	0.0653	2.85	0.0653	2.24
S2 site					
Benzene	400	0.0010	0.01	63.1160	2.01
	450	0.0010	0.01	6.7655	2.01
Propene	400	0.0724	2.07	0.0001	0.74
	450	0.0200	2.04	0.0001	0.01
S3 site					
Benzene	400	0.0075	0.99	0.0077	1.04
	450	0.1700	0.99	0.0016	1.01
Propene	400	0.0004	0.89	0.0038	5.20
	450	0.0009	6.03	0.0010	0.01

the temperature. The assumption of ideal adsorbed solution behavior, given by

$$P_i = P\mathrm{y}_i = P^{\circ}_{i,3}(\pi_3)x_{i,3} \tag{4}$$

gives the mixture composition.

The overall adsorbed phase composition is calculated by summing the amount of each species adsorbed on each site (Gusev and O'Brien 1996). The total amount adsorbed for the mixture in S3 site, $n_{t,3}$, is calculated by

$$\frac{1}{n_{t,3}} = \sum \frac{x_{i,3}}{\Theta^{\circ}_{i,3}(P^{\circ}_{i,3})} \tag{5}$$

where $\Theta^{\circ}_{i,3}(P^{\circ}_{i,3})$ is the number of moles of species i that would be adsorbed from the pure gas at $P^{\circ}_{i,3}(\pi)$. The number of moles of each species adsorbed in S3 site from the mixture, $n_{i,3}$ follows directly:

$$n_{i,3} = n_{t,3}x_i \tag{6}$$

However, adsorption in S1 site cannot be determined independently of the S3 site calculation but rather depends on both the composition and the amount of adsorption in S3 site (Gusev and O'Brien 1996). The amount adsorbed in S1

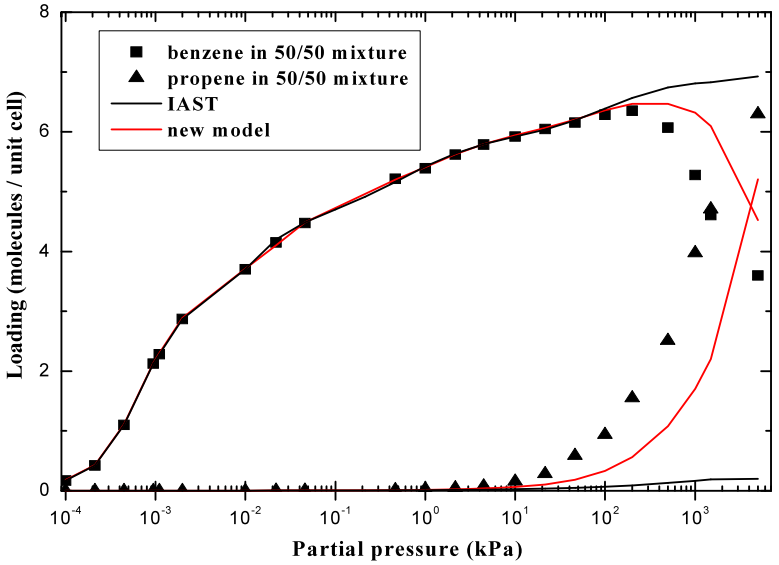

(a)

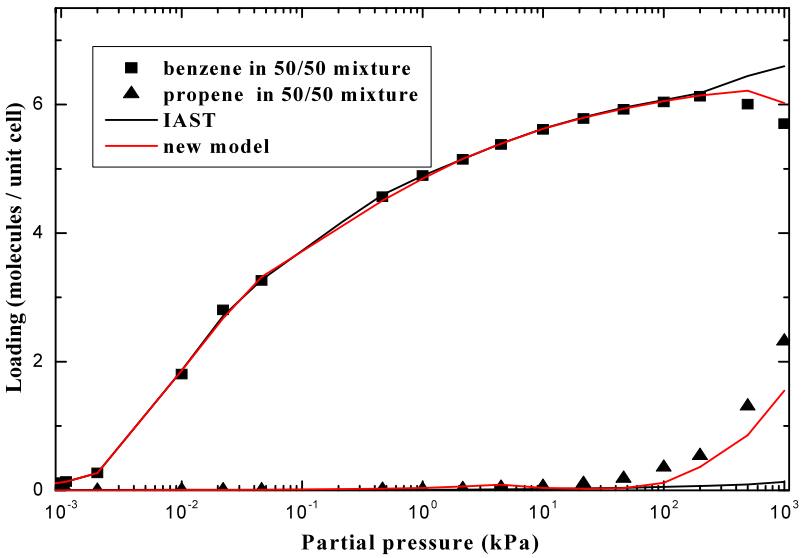

(b)

Fig. 9 IAST and the new model predictions compared with GCMC results. (**a**) 400 K; and (**b**) 450 K

site is scaled by the fractional occupancy of S3 site, $\eta_1(P)$, which is calculated by

$$\eta_1(P) = \sum \frac{n_{i,3}(P)}{a_{i,3}} \tag{7}$$

where $a_{i,3}$ is the saturation capacity of S3 site for species of i, which is shown in Table 6.

Equation (3) applied to adsorption in S1 site is written as:

$$\pi_1 = \frac{RT}{A}\int_{P=0}^{P=P_i^0} \eta_1(P)\frac{\Theta_{i,1}^{\circ}(P)}{P}dP \tag{8}$$

The amount adsorbed in S2 site is scaled by the summation of fractional occupancies of S3 and S1 sites, $\theta_3(P)$ and $\theta_1(P)$, which is calculated by

$$\begin{aligned}\eta_2(P) &= \sum(\theta_3(P) + \theta_1(P)) \\ &= \sum\left(\frac{n_{i,3}(P)}{a_{i,3}} + \frac{n_{i,1}(P)}{a_{i,1}}\right)\end{aligned} \tag{9}$$

where $a_{i,1}$ is the saturation capacity of S1 site for i species that is shown in Table 6. Equation (3) applied to adsorption in S2 site is written as:

$$\pi_2 = \frac{RT}{A}\int_{P=0}^{P=P_i^0} \eta_2(P)\frac{\Theta_{i,2}^{\circ}(P)}{P}dP \tag{10}$$

Finally, summing over the three sites gives the aggregate number of moles of each species adsorbed

$$\Theta_{t,i} = n_{i,1} + n_{i,2} + n_{i,3} \tag{11}$$

where, $n_{i,j}$ is the number of moles of each species adsorbed in j site from the mixture, which have been calculated respectively. $\Theta_{t,i}$ is the total adsorbed amount of species i.

The results are plotted in Fig. 9. As can be seen, at lower loadings, the IAST and the new model can all predict well for benzene and propene; however, at higher loadings, it is very evident that the new model have better performance than IAST. What is more, the selectivity reversal is not predicted by IAST. However, the new model is not perfect. The deviations between the new model predictions and the simulation results indicate that something is still missing in the model, such as steric exclusion of the larger molecules from micropores accessible to the smaller molecules. What is more, it is not very accurate that we assume the adsorption mechanism to be an analogous multilayer adsorption, which is the most important reason for the deviation. However, the new model has made a good attempt, and a relatively better result is attained than IAST.

4 Conclusions

In order to know the competition adsorption characteristics of benzene and propene in different pore systems of MCM-22, and how temperature, pressure and mole fraction can affect the adsorption results, Grand Canonical Monte Carlo simulation was used to calculate the mixture isotherms in different adsorption regions of MCM-22. The nine-site model of benzene was used, which have been proved effective and efficient. It is found that MCM-22 is sufficiently energetically heterogeneous for adsorption of benzene and propene, which is different from each other in size and adsorption energy. What is more, benzene and propene have the same preferential adsorption site and a similar adsorption order in different sites, which indicates that the two adsorbates follow the competition adsorption scenario proposed by Clark et al. (1998). A selectivity reversal of the mixture isotherms of benzene and propene is observed. Moreover, the situation is similar in the three adsorption sites which can be attributed to the energetic advantage of benzene at low loadings and entropy advantage of propene at high loadings in different sites. In addition, the competition adsorption in the three adsorption sites for the two adsorbates can fall into three successive steps. Moreover, the adsorption order of propene in mixture in these three sites is S3→S1→S2. A new model is presented to predict the benzene and propene adsorption equilibrium in MCM-22. This approach yields better multicomponent equilibrium predictions than IAST. In addition, with the increase of the mole fraction of benzene, the equilibrium ratio of benzene/propene in S1, S2 sits is quickly lower than 1 at a relatively lower feed ratio. However, the situation in S3 site is different, which indicate the necessity to improve the feed radio of benzene and propene.

Acknowledgements The financial supports by National Basic Research Program of China (973 program; No. 2010CB732301) and National Scientific Funding of China (No. 21046009) are gratefully acknowledged.

References

Asensi, M.A., Corma, A., Martínez, A.: Skeletal isomerization of 1-Butene on MCM-22 zeolite catalyst. J. Catal. **158**(2), 561–569 (1996)

Ayrault, P., Datka, J., Laforge, S., Martin, D., Guisnet, M.: Characterization of the internal and external acidity of H-MCM-22 zeolites. J. Phys. Chem. B **108**(36), 13755–13763 (2004)

Ban, S., Laak, A.V., Jongh, P.E.D., Eerden, J.P.J.M.V.D., Vlugt, T.J.H.: Adsorption selectivity of benzene/propene mixtures for various zeolites. J. Phys. Chem. C **111**, 17241–17248 (2007)

Calero, S., Dubbeldam, D., Krishna, R., Smit, B., Vlugt, T.J.H., Denayer, J.F.M., Martens, J.A., Maesen, T.L.M.: Understanding the role of sodium during adsorption: a force field for alkanes in sodium-exchanged faujasites. J. Am. Chem. Soc. **126**(36), 11377–11386 (2004)

Camblor, M.A., Corma, A., Diaz-Cabanas, M.-J., Baerlocher, C.: Synthesis and structural characterization of MWW type zeolite ITQ-1, the pure silica analog of MCM-22 and SSZ-25. J. Phys. Chem. B **102**(1), 44–51 (1998)

Chen, F., Deng, F., Cheng, M., Yue, Y., Ye, C., Bao, X.: Preferential occupation of xenon in zeolite MCM-22 as revealed by 129Xe NMR spectroscopy. J. Phys. Chem. B **105**(39), 9426–9432 (2001)

Chen, X., Huang, S., Cao, D., Wang, W.: Optimal feed ratio of benzene-propylene binary mixtures for alkylation in ZSM-5 by molecular simulation. Fluid Phase Equilib. **260**(1), 146–152 (2007)

Clark, L.A., Gupta, A., Snurr, R.Q.: Siting and segregation effects of simple molecules in zeolites MFI, MOR, and BOG. J. Phys. Chem. B **102**(35), 6720–6731 (1998)

Corma, A., Corell, C., Pérez-Pariente, J., Guil, J.M., Guil-López, R., Nicolopoulos, S., Calbet, J.G., Vallet-Regi, M.: Adsorption and catalytic properties of MCM-22: the influence of zeolite structure. Zeolites **16**(1), 7–14 (1996)

Corma, A., Martínez-Soriab, V., Schnoevelda, E.: Alkylation of benzene with short-chain olefins over MCM-22 zeolite: catalytic behaviour and kinetic mechanism. J. Catal. **192**(1), 163–173 (2000)

Degnan, T.F.J., Smith, C.M., Venkat, C.R.: Alkylation of aromatics with ethylene and propylene: recent developments in commercial processes. Appl. Catal. A, Gen. **221**(12), 283–294 (2001)

Frenkel, D., Smit, B.: Understanding Molecular Simulation: From Algorithms to Applications. Academic Press, New York (1996)

Fu, J., Ding, C.: Study on alkylation of benzene with propylene over MCM-22 zeolite catalyst by in situ IR. Catal. Commun. **6**(12), 770–776 (2005)

Gusev, V., O'Brien, J.A.: Theory for multicomponent adsorption equilibrium: multispace adsorption-model. Alchem. J. **42**(10), 2773–2783 (1996)

Hansen, N., Brüggemann, T., Bell, A.T., Keil, F.J.: Theoretical investigation of benzene alkylation with ethene over H-ZSM-5. J. Phys. Chem. C **112**(39), 15402–15411 (2008a)

Hansen, N., Krishna, R., van Baten, J.M., Bell, A.T., Keil, F.J.: Analysis of diffusion limitation in the alkylation of benzene over H-ZSM-5 by combining quantum chemical calculations, molecular simulations, and a continuum approach. J. Phys. Chem. C **113**(1), 235–246 (2008b)

Hou, T.J., Zhu, L.L., Li, Y.Y., Xu, X.J.: The localization and adsorption of benzene and propylene in ITQ-1 zeolite: grand canonical Monte Carlo simulations. J. Mol. Struct. **535**, 9–23 (2001)

Jakobtorweihen, S., Hansen, N., Keil, F.J.: Molecular simulation of alkene adsorption in zeolites. Mol. Phys. **103**(4), 471–489 (2005)

Jentys, A., Mukti, R.R., Tanaka, H., Lercher, J.A.: Energetic and entropic contributions controlling the sorption of benzene in zeolites. Microporous Mesoporous Mater. **90**(1–3), 284–292 (2006)

Jiíejka, Í.A.A.K., Ilkováa, N.D., Kotrlaa, J., Ernstb, S., Weber, A.: Activity and selectivity of zeolites MCM-22 and MCM-58 in the alkylation of toluene with propylene. Microporous Mesoporous Mater. **53**(1–3), 121–133 (2002)

Jorgensen, W.L., Madura, J.D., Swenson, C.J.: Optimized intermolecular potential functions for liquid hydrocarbons. J. Am. Chem. Soc. **106**(22), 6638–6646 (1984)

Krishna, R., Baten, J.M.V.: Influence of segregated adsorption on mixture diffusion in DDR zeolite. Chem. Phys. Lett. **446**(4–6), 344–349 (2007)

Liu, B., Smit, B., Rey, F., Valencia, S., Calero, A.S.A.: A new united atom force field for adsorption of alkenes in zeolites. J. Phys. Chem. C **112**, 2492–2498 (2008)

Maurer, R.T.: Multimodel approach to mixed-gas adsorption equilibria prediction. Alchem. J. **43**(2), 388–397 (1997)

Myers, A.L., Prausnitz, J.M.: Thermodynamics of mixed-gas adsorption. Alchem. J. **11**(1), 121–126 (1965)

Pawlesa, J., Zukal, A., Čejka, J.: Synthesis and adsorption investigations of zeolites MCM-22 and MCM-49 modified by alkali metal cations. Adsorption **13**(34), 257–265 (2007)

Perego, C., Ingallina, P.: Recent advances in the industrial alkylation of aromatics: new catalysts and new processes. Catal. Today **73**(12), 3–22 (2002)

Rungsirisakuna, R., Nanok, T., Probst, M., Limtrakul, J.: Adsorption and diffusion of benzene in the nanoporous catalysts FAU. ZSM-5 and MCM-22: a molecular dynamics study. J. Mol. Graph. Model. **24**(5), 373–382 (2006)

Sastre, G., Catlow, C.R.A., Corma, A.: Diffusion of benzene and propylene in MCM-22 zeolite a molecular dynamics study. J. Phys. Chem. B **103**(25), 5187–5196 (1999)

Schenk, M., Vidal, S.L., Vlugt, T.J.H., Smit, B., Krishna, R.: Separation of alkane isomers by exploiting entropy effects during adsorption on silicalite-1: a configurational-bias Monte Carlo simulation study. Langmuir **17**(5), 1558–1570 (2001)

Sircar, S.: Influence adsorbent of adsorbate size and heterogeneity on IAST. Alchem. J. **41**(5), 1135–1145 (1995)

Snurr, R.Q., Bell, A.T., Theodorou, D.N.: Prediction of adsorption of aromatic hydrocarbons in silicalite from grand canonical Monte Carlo simulations with biased insertions. J. Phys. Chem. **97**(51), 13742–13752 (1993)

Song, L., Sun, Z.-L., Ban, H., Dai, M., Rees, L.V.C.: Benzene adsorption in microporous materials. Adsorption **11**, 325–339 (2006)

Valenzuela, P.D., Myers, A.L.: Adsorption of gas mixtures: effect of energetic heterogeneity. Alchem. J. **34**(3), 397–402 (1998)

Vlugt, T.J.H., Schenk, M.: Influence of framework flexibility on the adsorption properties of hydrocarbons in the zeolite silicalite. J. Phys. Chem. B **106**(49), 12757–12763 (2002)

Wick, C.D., Siepmann, J.I., Klotzb, W.L., Schure, M.R.: Temperature effects on the retention of n-alkanes and arenes in helium–squalane gas–liquid chromatography: experiment and molecular simulation. J. Chromatogr. A **954**(1–2), 181–190 (2002)

Zhao, X.S., Chen, B., Karaborni, S., Siepmann, J.I.: Vapor−liquid and vapor−solid phase equilibria for united-atom benzene models near their triple points: the importance of quadrupolar interactions. J. Phys. Chem. B **109**(11), 5368–5374 (2005)

Zhu, X., Liu, S., Song, Y., Xie, S., Xua, L.: Catalytic cracking of 1-butene to propene ethene on MCM-22 zeolite. Appl. Catal. A, Gen. **290**(1–2), 191–199 (2005)